A Journal of the Gesellschaft Deutscher Chemiker

Angewandte International Edition GDCh Chemie

www.angewandte.org

Accepted Article

Title: A SARS-CoV-2 spike binding DNA aptamer that inhibits pseudovirus infection by an RBD independent mechanism

Authors: Günter Mayer, Anton Schmitz, Anna Weber, Mehtap Bayin, Stefan Breuers, Volkmar Fieberg, and Michael Famulok

To be cited as: *Angew. Chem. Int. Ed.* 10.1002/anie.202100316

Link to VoR: https://doi.org/10.1002/anie.202100316

WILEY-VCH

10.1002/anie.202100316

A SARS-CoV-2 spike binding DNA aptamer that inhibits pseudovirus infection by an RBD independent mechanism

Anton Schmitz[1,2 †], Anna Weber[1,3 †], Mehtap Bayin[1,2], Stefan Breuers[1,3], Volkmar Fieberg[1,2], Michael Famulok[1,2,3 *], and Günter Mayer[1,3 *]

[1] Life and Medical Sciences (LIMES), University of Bonn, Gerhard-Domagk-Str.1, Germany
[2] Max Planck Fellow Chemical Biology, Center of Advanced European Studies and Research (caesar), Ludwig-Erhard-Allee 2, Bonn 53175, Germany
[3] Center of Aptamer Research & Development, University of Bonn, Gerhard-Domagk-Str. 1, 53121 Bonn, Germany
*Corresponding authors: gmayer@uni-bonn.de, m.famulok@uni-bonn.de
† these authors contributed equally

Abstract

The receptor binding domain (RBD) of the spike glycoprotein of the coronavirus SARS-CoV-2 (CoV2-S) binds to the human angiotensin converting enzyme 2 (ACE2) representing the initial contact point for leveraging the infection cascade. We used an automated selection process and identified an aptamer that specifically interacts with CoV2-S. The aptamer does not bind to the RBD of CoV2-S and does not block the interaction of CoV2-S with ACE2. Notwithstanding, infection studies revealed potent and specific inhibition of pseudoviral infection by the aptamer. The present study opens up new vistas in developing SARS-CoV2 infection inhibitors, independent of blocking the ACE2 interaction of the virus and harnesses aptamers as potential drug candidates and tools to disentangle hitherto inaccessible infection modalities, which is of particular interest in light of the increasing number of escape mutants that are currently being reported.

Introduction

The coronavirus SARS-CoV-2 binds via its spike protein (CoV2-S) to the extracellular domain of the human angiotensin-converting enzyme 2 (ACE2) initiating the entry process into target cells. CoV2-S is a trimeric, highly glycosylated class I fusion protein. It binds to ACE2 via the receptor binding domain (RBD) of its S1 subunit.[1] The trimeric spike exists in a closed form which does not interact with ACE2 and in an open form where one RBD is in the so-called 'up' conformation exposing the ACE2 binding site.[2,3] Upon RBD binding to ACE2 the interaction between the S1 and S2 subunits is weakened allowing S2 to undergo substantial structural rearrangements to finally fuse the virus with the host cell membrane.[2,3] The important role of

10.1002/anie.202100316

the RBD for viral infectivity is underlined by the analyses of neutralizing antibodies from sera of human re-convalescents, which reveal binding of these antibodies to RBD.[4,5] Consequently, almost all published neutralizing antibodies developed for therapeutic use target RBD, including humanized monoclonal antibodies[6], antibodies cloned from human B cells[7-9] and single-chain camelid antibodies.[10,11] However, mutations in RBD of CoV2-S can cause RBD-targeted antibodies ineffectual while the virus's interaction with ACE2 remains unchanged or even found improved.[12] To address this limitation, additional inhibitors of viral infection and a different mode of action, e.g., by targeting other domains of CoV2-S are highly desired but of limited availability.

Against this backdrop, we here report on a DNA aptamer with a different modality of inhibiting viral infection. As the aptamer does not interact with RBD, it does not interfere with the binding of CoV2-S to ACE2. Regardless, the aptamer inhibits viral infection, exemplified by employing a CoV2-S pseudotyped virus and an ACE2 expressing cell line. These findings demonstrate that viral infection can be inhibited independent of targeting RBD and suggest that inhibition could be possible despite the virus has already bound to cells. The results open the path to inhibitors of SARS-CoV-2 infection with hitherto inaccessible modes of action.

RESULTS

Selection and characterization of CoV2-S binding aptamers

To identify single-stranded (ss)DNA aptamers that bind to CoV2-S we employed an automated selection procedure[13]. The trimerized His-tagged extracellular domain of CoV2-S, stabilized in the prefusion conformation, was expressed and purified from HEK293 cells[14,15] and immobilized for the selection on magnetic beads. After twelve selection cycles (**Supporting Fig. 1a**) the enriched ssDNA libraries were analyzed for improved CoV2-S binding by flow cytometry using cy5-labelled ssDNA and CoV2-S immobilized on magnetic particles (**Fig. 1a**). These experiments revealed an increased fluorescence signal of the ssDNA from selection cycle 12 in the presence of CoV2-S (**Fig. 1a**). No interaction was observed when particles without CoV2-S or particles modified with His6-Erk2 or His6-dectin-1 were used, indicating specificity of the enriched ssDNA library. In contrast, the ssDNA library from selection cycle 1 did not show interaction with the particles, independent of their modification state (**Fig. 1a**). The enriched DNA populations were subjected to next-generation sequencing (NGS), in which 10^6 to10^7 sequences were analyzed per selection cycle (**Supporting Fig. 1b**). This analysis revealed a strong decrease in the number of unique DNA sequences, starting from selection cycle 4 and levelling between 10% to 5% of unique DNA sequences in selection cycle 7 to 12 (**Fig. 1b**).

10.1002/anie.202100316

Likewise, the distribution of nucleotides within the initial random region changed significantly throughout the course of selection, in which guanine is the most frequently enriched nucleotide (**Supporting Fig. 1c**). These data reveal a strong enrichment of DNA sequences, which is further supported by the occurrence of sequences with high copy numbers, e.g., > 100.000 per sequence starting from the DNA populations from selection cycle 5 onwards (**Fig. 1c**). Further in-depth population analysis revealed the occurrence of sequence families, termed family 8, 13, 22, 29, and 30 (**Fig. 1d**, **Supporting Fig. 1d**, **Supporting Table 1**). Whereas the frequency of sequences belonging to family 8 started to enrich from cycle 8 onwards, all other families were observed in the DNA populations from selection cycles 4 to 6, having maximum frequency between selection cycles 7 to 10 and declined afterwards (**Fig. 1d**). We chose representative monoclonal sequences within each family that reflect the enrichment patterns (SP1-7, **Fig. 1e**) and tested them regarding interaction with CoV2-S using flow cytometry. These studies revealed interaction of the family 8 sequences SP5, SP6, SP7 with CoV2-S (**Fig. 1f,g**). All other sequences and a scrambled version of SP5 (SP5sc) as putative non-binding negative control sequence did not interact with the target protein (**Fig. 1f**). SP5, SP6, and SP7 bind with high specificity to CoV2-S; no binding to the isolated RBD, ACE2 or to the spike protein of SARS-CoV (CoV-S) was observed (**Fig. 1h**). Kinetic analysis by surface plasmon resonance (SPR) of the interaction of CoV2-S with 5'-biotinylated aptamer variants immobilized on streptavidin coated sensor surfaces show high affinity binding to CoV2-S, with dissociation constants (K_D) between 9 and 21 nanomolar (**Tab. 1**, **Supporting Fig. 2a,b**). All aptamers revealed comparable K_D values at 37°C vs. 25°C (**Tab. 1**). A qualitative assay[16] to determine the impact of the 5'-modifications on the aptamers CoV2-S binding properties revealed only minor influence of the 5'-cy5-, 5'-biotin-, or 5'-hydroxyl labels (**Supporting Fig. 2c**). SP5 showed a slightly decreased binding in the hydroxyl state whereas binding of SP6 to CoV2-S was found to increase by ~50% in the unmodified state as compared to the 5'-cy5-modified version (**Supporting Fig. 2c**). The interaction properties of SP7 appeared to be independent of 5'-modifications (**Supporting Fig. 2c**).

SP6 as a representative of the family 8 was chosen for further analysis (**Fig. 1g**). Based on secondary structure predictions (**Supporting Fig. 2d**), the aptamer was initially truncated, yielding SP6.51, and analyzed by flow cytometry for CoV2-S binding. Interestingly, SP6.51 showed strongly improved binding compared to the parental SP6 aptamer (**Fig. 1i**). Further truncation of SP6, yielding variants with 45 nucleotides (nt, SP6.45), 41 nt (SP6.41), or 34 nt (SP6.34) maintained the elevated binding properties. When SP6 was truncated to 30 nt (SP6.30) binding fell back to the level of the original SP6 aptamer whereas the interaction with CoV2-S

10.1002/anie.202100316

was entirely lost by removing additional 11nt (SP6.19, **Fig. 1i**, **Supporting Fig. 2d**). Moreover, based on the secondary structure prediction of SP6.34, we investigated the interaction of the point mutants of the minimal aptamer variant SP6.34, namely SP6.34A, SP6.34G and SP6.34C with CoV2-S by flow cytometry. These point mutants were chosen to either stabilize (SP6.34C) or destabilize (SP6.34A, SP6.34G) the putative apical stem structure (**Fig. 1j**). However, all point mutants revealed severely diminished binding to CoV2-S, whereas binding of SP6.34A was still detectable (**Fig. 1i**), albeit to a much lesser extent than SP6. Mutating the positions equivalent to SP6.34C in the parental aptamer SP6, yielding SP6C, also abolishes CoV2-S binding (**Fig. 1k**). To conclude the characterization of SP6, the impact of mono- and divalent ions on CoV2-S binding was assessed by flow cytometry of both, the parental and minimal variant of the aptamer. These studies reveal that the binding of SP6 to CoV2-S is sensitive towards the presence of K^+ and strongly depends on Mg^{2+}-ions (**Fig. 1k**). The binding of the parental aptamer SP6 to CoV2-S was maintained in the absence of K^+-ions, whereas the interaction of the minimal variant SP6.34 was found to be reduced by about 50% compared to its level obtained in PBS (**Fig. 1k**). These data indicate that K^+-ions are most likely required for supporting structure formation of the aptamer, which is more pronounced in the truncated variant than in the parental full-length aptamer, but not essential for CoV2-S binding.

10.1002/anie.202100316

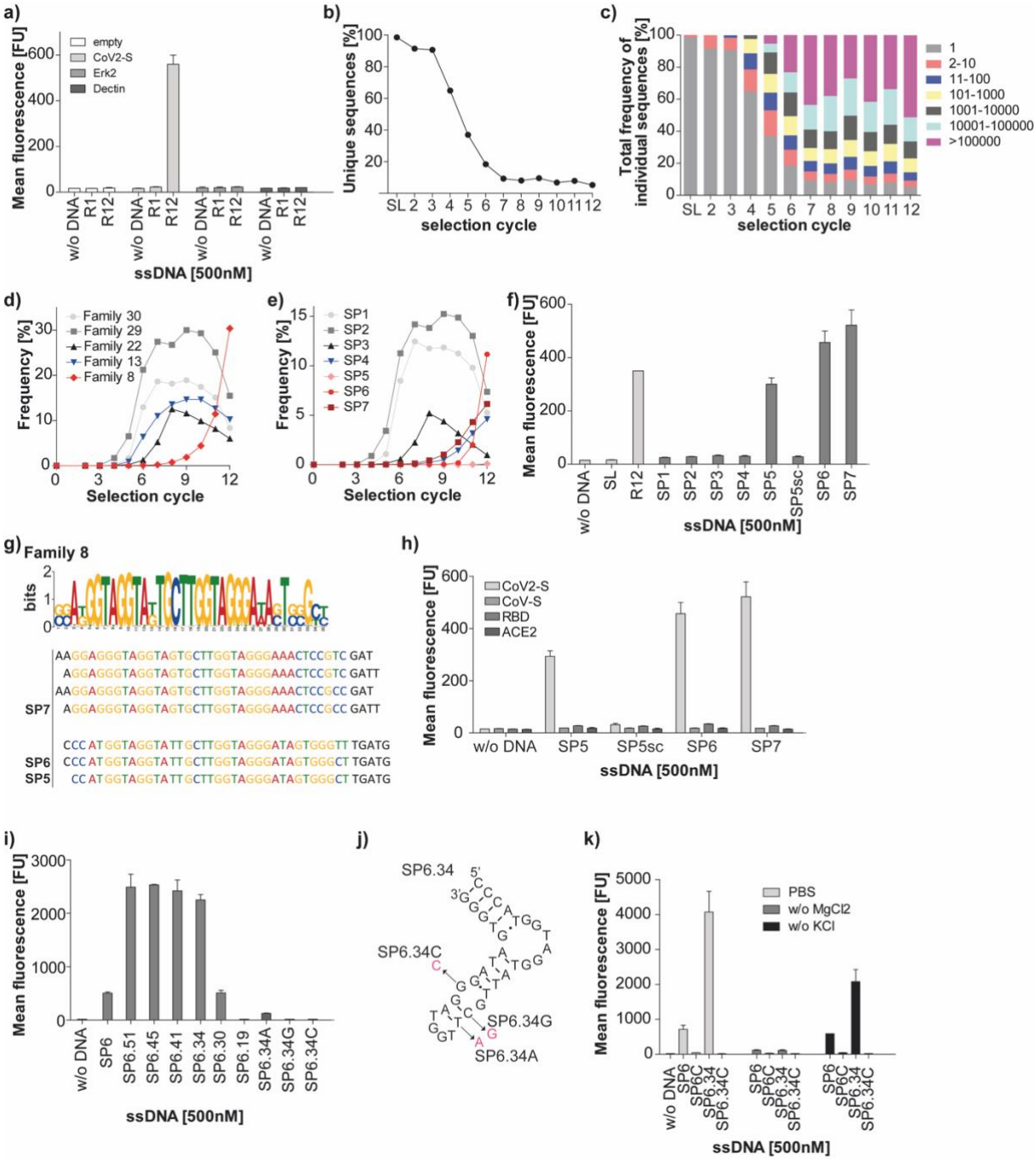

Figure 1: Selection of DNA aptamers binding to CoV2-S. a) Interaction analysis of the enriched DNA library from selection cycle 1 (R1) and 12 (R12) in respect to empty beads, CoV2-S, Erk2 and Dectin. **b)** Amount of unique sequences in the DNA populations from selection cycle 1-12 and the starting library (SL). c) Fraction of sequences in the DNA population from selection cycle 1-12 and the starting library (SL) sharing the indicated copy numbers. **d)** Frequency of sequences throughout the DNA population from selection cycles 0-12 belonging to the sequence families 8, 13, 22, 29, or 30. See also Supporting Fig. 1d. **e)** Frequency of representative sequences belonging to one of the families from (**d**). SP1 (Fam 30), SP2 (Fam 29), SP3 (Fam 22), SP4 (Fam 13), SP5-7 (Fam 8). **f)** Interaction analysis of aptamers SP1-7, the starting library (SL) and DNA from selection cycle 12 (R12) with CoV2-S. SP5sc: scrambled control sequence with identical nucleotides as SP5 but with different primary structure. g) Sequence motif of family 8 and assignment of aptamers SP5-7. **h)** Interaction analysis of the scrambled sequence SP5sc and aptamers SP5-7 with CoV2-S, RBD, ACE2, and CoV-S. **i)** Interaction analysis of SP6 and shortened

variants and defined single point mutants thereof (**j**). **k)** Interaction analysis of SP6, SP6.34 and the respective control aptamers SP6C (see supporting Fig. 2d) and SP6.34C (**j**) with CoV2-S in the absence and presence of Mg^{2+}-ions or K^{+}-ions. a,f, h,i, and k: N=2, mean +/- SD.

Aptamers selected for the RBD do not interact with CoV2-S

We also performed automated selection procedures to target the isolated RBD of Cov2-S (**Supporting Fig. 3**). Conventional automated selection conditions, as applied targeting CoV2-S (**Fig. 1**), resulted in strong overamplification during the PCR step (**Supporting Fig. 3a**), which could be decreased by reducing the amount of target (10% compared to the conventional approach, **Supporting Fig. 3b**) or by adding heparin as a competitor during the incubation step of the selection procedure (**Supporting Fig. 3c**). Interaction analysis of the obtained DNA libraries from the selection cycles in which no or very low overamplification was observed, i.e. cycle 6 of the conventional procedure (**Supporting Fig. 3a**), cycle 9 when less target was used (**Supporting Fig. 3b**), and cycle 8 when heparin was added (**Supporting Fig. 3c**), revealed enrichment of RBD binding species in all selections (**Supporting Fig. 3d**). However, none of the enriched RBD-binding libraries interacted with full-length CoV2-S comprising the complete extracellular domain (**Supporting Fig. 3d**). The starting library, used as negative control, neither bound to RBD nor to CoV2-S, whereas the library enriched for CoV2-S (R12 CoV2-S, **Fig. 1a**), used as positive control, showed binding to CoV2-S as expected (**Supporting Fig. 3d**). Of note, library R12 CoV2-S also revealed interaction with RBD, although to a lesser extent than to CoV2-S (**Supporting Fig. 3d**). Therefore, we decided to use the library R12 CoV2-S to conduct three additional selection cycles (cycles 13-15) enriching for those species that bind predominantly to RBD instead of other domains of CoV2-S, that are presumably targeted by SP5, SP6, and SP7 (**Fig. 1h**). We again used the conventional selection approach (cycles 13-15, **Supporting Fig. 3e**) and a selection variant with less (10%) RBD than in the preceding selection (cycles 13*-15*, **Supporting Fig. 3e**). In both cases overamplification was observed from cycle 13/13* on, although less pronounced as during the *de novo* selection targeting RBD under previously applied selection conditions (**Supporting Fig. 3a**). Both enriched libraries (R15/R15*) showed binding to RBD but no interaction with CoV2-S (**Supporting Fig. 3f**). Next-generation sequencing of the obtained libraries revealed two strongly enriched distinct families (**Supporting Fig. 3g-i**, **Supporting Tables 2,3**). We chose four representative sequences, RBD1-4, and performed interaction analysis. These experiments were found to be in-line with the observations obtained with the enriched libraries, i.e. the sequences bound to RBD (**Supporting Fig. 3j**) but not CoV2-S (**Supporting Fig. 3k**). Despite RBD4, which was found at elevated copy numbers in selection cycle 6 of the selection

10.1002/anie.202100316

targeting CoV2-S but declining thereafter, all RBD binding sequences only increased in copy numbers when the target changed from CoV2-S to RBD in selection cycles 13-15 (**Supporting Fig. 3l**) and 13* to 15* (**Supporting Fig. 3m**). These data indicate that targeting RBD of CoV2-S with DNA libraries, in our hands, was not productive in yielding aptamers interacting with the full-length extracellular domain of CoV2-S protein *in vitro*. We analyzed also the interaction properties of the previously described DNA aptamers RBD C1 and RBD C4, which were selected for binding to RBD. [17] Unfortunately, in our assay we could neither observe binding of the aptamers to RBD nor to CoV-2S (**Supporting Fig. 4**).

SP6 inhibits viral infection independent of the interaction of CoV2-S with ACE2

We next performed pulldown experiments to further characterize and verify the interaction of SP6 with CoV2-S (**Fig. 2a**). In these experiments, biotinylated SP6 or SP6C were incubated with the respective protein and the complexes were collected by adding streptavidin coated magnetic beads. After washing, the remaining proteins were analyzed by SDS-PAGE and Coomassie staining of the gel. Aliquots were taken and analyzed prior to the incubation with the magnetic beads (input, **Fig. 2a**), from the supernatant after incubation with the magnetic beads (unbound, **Fig. 2a**) and from the bead/aptamer bound fraction (eluate, **Fig. 2a**). SP6 revealed binding to CoV2-S (**Fig. 2a**, eluate, lane 2) but not to CoV-S (eluate, lane 6) nor to ACE2 (eluate, lane 4) or the unrelated control protein Nek7 (eluate, lane 5). In this experiment, SP6C showed weak binding to CoV2-S (**Fig. 2a**, eluate, lane 1). In agreement with the results obtained by flow cytometry (**Fig. 1h**) binding of SP6 to CoV2-S was not reduced even in the presence of a fivefold molar excess of RBD (**Fig.2a**, eluate, lane 3).

As SP6 appears not to interact with the RBD of CoV2-S, we investigated whether SP6 has an impact on the interaction of CoV2-S and ACE2. To this end, His-tagged CoV2-S was pulled by Ni-NTA magnetic beads and the co-pulldown of untagged ACE2 (ACE2ΔHis) was analyzed in the presence or absence of SP6 (**Fig. 2b**). As before, input, unbound and eluate fractions were analyzed by SDS-PAGE and Coomassie staining. Whereas the interaction between CoV2-S and ACE2 was abolished by the RBD-binding control nanobody VHH E[18] (**Fig. 2b**, eluate, lane 4), SP6 did not affect this interaction (eluate, lane 3). Densitometric analysis of the respective bands resulted in ACE2:Cov2-S ratios of 0.18 and 0.16 in the absence (eluate, lane 1) or presence (eluate, lane 3) of SP6, respectively. To further substantiate this finding, complex formation between CoV2-S-RBD and ACE2 was monitored by analytical size exclusion chromatography (**Supporting Fig. 5**). Again, complex formation was prevented by VHH E but was unaffected by SP6.

10.1002/anie.202100316

Having shown SP6 interacts with CoV2-S without interfering with complex formation with its cellular receptor ACE2, we next studied the impact of SP6 on viral infection. To address this question, we used the established VSV-ΔG*-based pseudotype system[19,20] and generated Cov2-S and VSV-G pseudotyped virus particles. The interaction of SP6 with the CoV2-S pseudotyped virus was verified by an enzyme-linked oligonucleotide assay (ELONA).[21] In this experiment, the CoV2-S protein or the CoV2-S pseudotyped virus were captured by a nanobody binding to the RBD of CoV2-S and after washing the bound protein or pseudovirus particles were detected by adding biotinylated SP6, streptavidin-horse radish peroxidase (HRP) conjugates and its substrate 2,2′-Azino-di(3-ethylbenzthiazoline-6-sulfonic acid) (ABTS) (**Supporting Fig. 6**). We observed a concentration dependent increase in signal when SP6 and SP6.34 were used for detection, but not when employing SP6C and SP6.34C (**Supporting Fig. 6a**). Likewise, SP6 but not SPC6C detected the CoV2-S pseudotyped virus. The VSV-G pseudotype was not detected demonstrating the specificity of the assay (**Fig 2c**). Next, ACE2-expressing Vero E6 cells were infected with Cov2-S or VSV-G pseudotyped virus particles, which had been pre-incubated with SP6 or SP6C (**Fig. 2c**). Pseudotype particle numbers were adjusted to result in infection rates between 8 % and 10 % for the aptamer-untreated pseudotypes (**Supporting Fig. 6b,c**). This infection rate was chosen to prevent multiple infections of a single cell precluding reliable measurements. SP6 showed a concentration-dependent reduction of infection of Vero E6 cells by the CoV2-S pseudotype virus (**Fig. 2d**, **Supporting Fig. 6b,c**). In contrast, the infection of the VSV-G pseudotype was not affected (**Fig. 2d**). These results demonstrate the dependence of the inhibitory effect of SP6 on the presence of CoV2-S on the viral particles and exclude unspecific effects on the infection process of the VSV-G vector. The presence of SP6C also led to some reduction of infection which, however, did not reach statistical significance. The seeming discrepancy to the lack of binding of SP6C to CoV2-S in the binding assay (**Fig. 1k**) or the ELONA (**Fig. 2c**) is explained by the higher concentrations of SP6C used in the infection assay. In addition, unmodified SP6 (as used in the infection assay) shows stronger binding to CoV2-S than the 5´-modified versions (**Supporting Fig. 2c**) and this can also be assumed for SP6C. The slight inhibitory effect of SP6C is in-line with its observed weak interaction with CoV2-S in the pulldown assay (**Fig. 2a**).

Whereas ACE2 is the most important receptor for CoV2-S, at least two co-receptors are known to contribute to CoV2-S binding to target cells, heparan sulfate and neuropilin-1.[22,23] Therefore, we investigated whether SP6 affected binding of CoV2-S pseudotyped particles to cells even if it did not inhibit CoV2-S binding to ACE2. For this purpose, VSV-ΔG* was

10.1002/anie.202100316

pseudotyped with CoV2-S carrying a HiBiT tag at the C-terminus. Vero E6 cells were incubated with these particles and bound virus was quantified by NanoBiT reconstitution (**Fig 2e**). Whereas the known inhibitor heparin[24] reduced binding of CoV2-S pseudotyped particles, neither SP6 nor SP6C had an effect on binding. These data show that SP6 reduces pseudovirus infection by interfering with a process occurring after binding of the pseudovirus to cells.

10.1002/anie.202100316

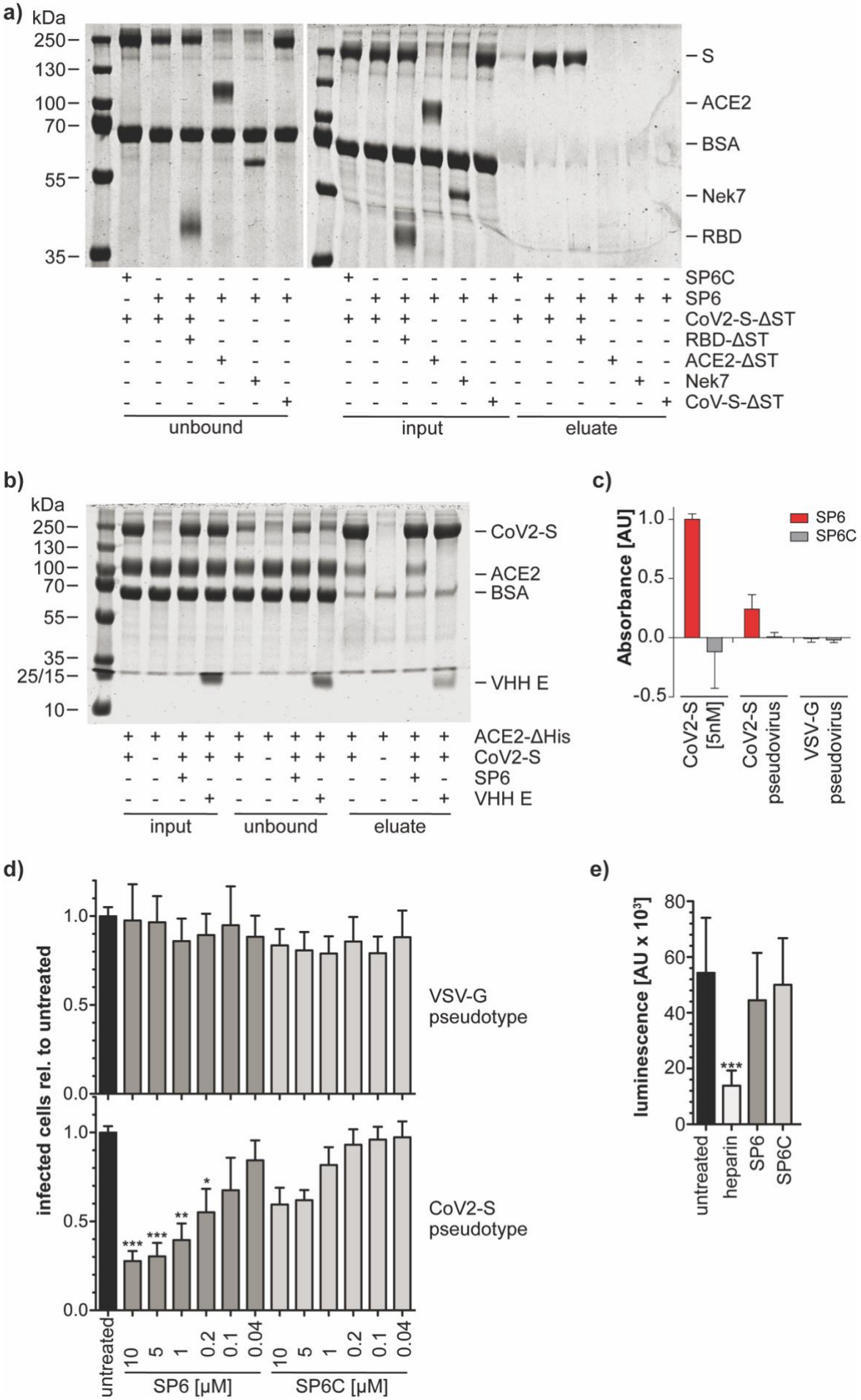

10.1002/anie.202100316

Figure 2: RBD independent inhibition of CoV2-S pseudovirus infection. a) Pulldown analysis of SP6 binding specificity. ΔST indicates constructs lacking the StrepTag. **b)** Pulldown analysis of CoV2-S ACE2 interaction. ΔHis indicates lack of His tag. **c)** ELONA of S protein and SARS-CoV-2-S pseudotype virus. **d)** SARS-CoV-2-S pseudovirus infection. n=5, mean +/- SD, *** p<0.001, ** p<0.01, * p<0.05. **e)** SARS-CoV-2-S pseudovirus binding. n=8, mean +/- SD *** p<0.001

Discussion

In conclusion, we describe the DNA aptamer SP6 binding to CoV2-S and with the potential to inhibit SARS-CoV-2 infection. A remarkable and unexpected feature of SP6 is that its inhibitory effect does not result from interfering with the interaction of CoV2-S with ACE2. This feature distinguishes the mode of action of SP6 from that of CoV2-S targeting antibodies. Currently, the overwhelming majority of these antibodies bind to the RBD of CoV2-S[6-11] and prevent ACE2 interaction by either directly competing with ACE2 for binding[6-10] or by stabilizing an ACE2 binding-incompetent conformation[11]. Antibodies not binding to RBD but to the N-terminal domain of CoV2-S have also been shown to prevent interaction of CoV2-S with ACE2 although by an yet unknown mechanism.[10] To our knowledge, neutralizing antibodies targeting the S2 domain have not yet been described. At present, the molecular mechanism by which SP6 inhibits viral infection is unknown. As the binding of CoV2-S pseudotypes to cells is not affected, we conclude that a step occurring after binding must be impeded. This could involve preventing S2´ cleavage or destabilizing the prefusion conformation of the spike protein. The latter mechanism has been shown to lead to viruses bearing spike proteins in the postfusion conformation and has been reported for an antibody neutralizing SARS-CoV.[25] This antibody, however, binds to the RBD. We anticipate that the elucidation of the mechanism by which SP6 inhibits infection will provide insight into how CoV2-S triggers fusion of the viral and host cell membranes. While this submission was under review, a related study was published describing aptamers that bind to the RBD domain of CoV2-S and inhibit pseudoviral infection by a mechanism distinct to the one of SP6. [26]

There is an increasing number of currently reported mutations in SARS-CoV-2[9], among which the most recent example is the apparently faster spreading lineage VUI-202012/01, also named B.1.1.7.[27] This variant shows several mutations in the RBD resulting in escape of binding to some antibodies. Since more escape mutations in the RBD can be expected to further arise in the future, RBD-independent modalities to prevent infection, as revealed by SP6, are of relevance and need to be investigated. Along these lines, testing the ability of the SP6 to inhibit isolates of SARS-CoV-2 and subsequent *in vivo* infection studies are next steps to further develop and validate the aptamer's therapeutic potential.

10.1002/anie.202100316

SP6 might be further optimized to increase potency. For example, homo- or heterovalent multimers could be engineered by combining SP6 with itself or aptamers (or other ligands) binding to different CoV2-S domains, a strategy employed previously to gain very potent thrombin inhibitors.[28,29] Indeed, di- or trimerization of CoV2-S antibodies has been shown to increase their potency.[11,30] The automated selection process enables the rapid generation of aptamers, for example for mutated proteins of SARS-CoV-2 lineages that escape treatment regimens by aptamers, antibodies, or other active pharmaceutical ingredients. Likewise, re-selection strategies to adapt SP6 towards mutations are also possible. In addition to these features, aptamers provide means to develop antigen tests, exemplified by the presented SP6-based ELONA data. The ease by which aptamers can be synthesized, their low batch-to-batch variations and long shelf lives predestines SP6 for various diagnostic and treatment options, e.g., as inhalation spray.

Acknowledgement

This work has been made possible by funds from the Federal Ministry of Education and (BMBF, 01KI20154 to MF and GM) and by the German Research Council (DFG, MA3442/7-1 to GM). We thank Dr. F.-I. Schmidt and Dr. P.-A. König (Core Facility Nanobodies, Medical Faculty, University of Bonn) for providing the RBD nanobody, Prof. O. Stemmann (University of Bayreuth) for the Dye488-labelled RBD and Prof. J. Schultze for performing NGS (University of Bonn/DZNE). We are grateful to Dr. G. Zimmer (Institute of Virology and Immunology, Mittelhäusern, Switzerland) for providing the VSV-ΔG* and to Prof. J.S. McLellan (The University of Texas at Austin, USA) for providing the plasmid for CoV2-S expression.

Author contribution

AS developed the cellular binding and partly executed the cellular binding and infection assays, constructed the pseudotype viruses and wrote the manuscript. AW performed sequence analysis of the enriched libraries and conducted interaction analysis of the DNA libraries, aptamers and their variants. MB conducted infection and binding experiments. SB performed the automated selection experiments. VF expressed and purified proteins and performed the pulldown experiments. MF supervised experiments, discussed results and wrote the manuscript. GM conceived and designed the study, supervised and discussed results and wrote the manuscript. All authors have read and commented on the manuscript.

Competing interests

AS, AW, SB, VF, MF and GM are listed as inventors on a pending patent application on the aptamers described in this study.

References

[1] M. M. Hatmal, W. Alshaer, M. A. I. Al-Hatamleh, M. Hatmal, O. Smadi, M. O. Taha, A. J. Oweida, J. C. Boer, R. Mohamud, M. Plebanski, *Cells* **2020**, *9*, 2638.

[2] D. J. Benton, A. G. Wrobel, P. Xu, C. Roustan, S. R. Martin, P. B. Rosenthal, J. J. Skehel, S. J. Gamblin, *Nature* **2020**, *588*, 327–330.

[3] Y. Cai, J. Zhang, T. Xiao, H. Peng, S. M. Sterling, R. M. Walsh, S. Rawson, S. Rits-Volloch, B. Chen, *Science* **2020**, *369*, 1586–1592.

[4] D. F. Robbiani, C. Gaebler, F. Muecksch, J. C. C. Lorenzi, Z. Wang, A. Cho, M. Agudelo, C. O. Barnes, A. Gazumyan, S. Finkin, et al., *Nature* **2020**, *584*, 437–442.

[5] C. O. Barnes, A. P. West, K. E. Huey-Tubman, M. A. G. Hoffmann, N. G. Sharaf, P. R. Hoffman, N. Koranda, H. B. Gristick, C. Gaebler, F. Muecksch, et al., *Cell* **2020**, *182*, 828–842.e16.

[6] C. Wang, W. Li, D. Drabek, N. M. A. Okba, R. van Haperen, A. D. M. E. Osterhaus, F. J. M. van Kuppeveld, B. L. Haagmans, F. Grosveld, B.-J. Bosch, *Nat Commun* **2020**, *11*, 2251–6.

[7] B. Ju, Q. Zhang, J. Ge, R. Wang, J. Sun, X. Ge, J. Yu, S. Shan, B. Zhou, S. Song, et al., *Nature* **2020**, *584*, 115–119.

[8] R. Shi, C. Shan, X. Duan, Z. Chen, P. Liu, J. Song, T. Song, X. Bi, C. Han, L. Wu, et al., *Nature* **2020**, *584*, 120–124.

[9] L. Liu, P. Wang, M. S. Nair, J. Yu, M. Rapp, Q. Wang, Y. Luo, J. F.-W. Chan, V. Sahi, A. Figueroa, et al., *Nature* **2020**, *584*, 450–456.

[10] J. Huo, A. Le Bas, R. R. Ruza, H. M. E. Duyvesteyn, H. Mikolajek, T. Malinauskas, T. K. Tan, P. Rijal, M. Dumoux, P. N. Ward, et al., *Nat. Struct. Mol. Biol.* **2020**, *27*, 846–854.

[11] M. Schoof, B. Faust, R. A. Saunders, S. Sangwan, V. Rezelj, N. Hoppe, M. Boone, C. B. Billesbølle, C. Puchades, C. M. Azumaya, et al., *Science* **2020**, *370*, 1473–1479.

[12] Q. Li, J. Wu, J. Nie, L. Zhang, H. Hao, S. Liu, C. Zhao, Q. Zhang, H. Liu, L. Nie, et al., *Cell* **2020**, *182*, 1284–1294.e9.

[13] S. Breuers, L. L. Bryant, T. Legen, G. Mayer, *Methods* **2019**, *161*, 3–9.

[14] D. Wrapp, N. Wang, K. S. Corbett, J. A. Goldsmith, C.-L. Hsieh, O. Abiona, B. S. Graham, J. S. McLellan, *Science* **2020**, *367*, 1260–1263.

[15] C.-L. Hsieh, J. A. Goldsmith, J. M. Schaub, A. M. DiVenere, H.-C. Kuo, K. Javanmardi, K. C. Le, D. Wrapp, A. G. Lee, Y. Liu, et al., *Science* **2020**, *369*, 1501–1505.

[16] A. M. Weber, J. Kaiser, T. Ziegler, S. Pilsl, C. Renzl, L. Sixt, G. Pietruschka, S. Moniot, A. Kakoti, M. Juraschitz, et al., *Nat. Chem. Biol.* **2019**, *15*, 1085–1092.

[17] Y. Song, J. Song, X. Wei, M. Huang, M. Sun, L. Zhu, B. Lin, H. Shen, Z. Zhu, C. Yang, *Anal. Chem.* **2020**, *92*, 9895–9900.

[18] P.-A. Koenig, H. Das, H. Liu, B. M. Kümmerer, F. N. Gohr, L.-M. Jenster, L. D. J. Schiffelers, Y. M. Tesfamariam, M. Uchima, J. D. Wuerth, et al., *Science* **2021**, eabe6230.

[19] M. Berger Rentsch, G. Zimmer, *PLoS ONE* **2011**, *6*, e25858.

[20] F. Zettl, T. L. Meister, T. Vollmer, B. Fischer, J. Steinmann, A. Krawczyk, P. V'kovski, D. Todt, E. Steinmann, S. Pfaender, et al., *Vaccines (Basel)* **2020**, *8*, 386.
[21] D. W. Drolet, L. Moon-McDermott, T. S. Romig, *Nat. Biotechnol.* **1996**, *14*, 1021–1025.
[22] T. M. Clausen, D. R. Sandoval, C. B. Spliid, J. Pihl, H. R. Perrett, C. D. Painter, A. Narayanan, S. A. Majowicz, E. M. Kwong, R. N. McVicar, et al., *Cell* **2020**, *183*, 1043–1057.e15.
[23] L. Cantuti-Castelvetri, R. Ojha, L. D. Pedro, M. Djannatian, J. Franz, S. Kuivanen, F. van der Meer, K. Kallio, T. Kaya, M. Anastasina, et al., *Science* **2020**, *370*, 856–860.
[24] R. Tandon, J. S. Sharp, F. Zhang, V. H. Pomin, N. M. Ashpole, D. Mitra, M. G. McCandless, W. Jin, H. Liu, P. Sharma, et al., *J Virol* **2020**, DOI 10.1128/JVI.01987-20.
[25] A. C. Walls, X. Xiong, Y.-J. Park, M. A. Tortorici, J. Snijder, J. Quispe, E. Cameroni, R. Gopal, M. Dai, A. Lanzavecchia, et al., *Cell* **2019**, *176*, 1026–1039.e15.
[26] M. Sun, S. Liu, X. Wei, S. Wan, M. Huang, T. Song, Y. Lu, X. Weng, Z. Lin, H. Chen, et al., *Angew. Chem. Int. Ed. Engl.* **2021**, DOI 10.1002/anie.202100225.
[27] *Microsoft Word - Report 1_COG-UK_20 December 2020_SARS-CoV-2 Mutations_Final.Docx*, **2020**.
[28] J. Müller, B. Wulffen, B. Pötzsch, G. Mayer, *Chembiochem* **2007**, *8*, 2223–2226.
[29] Y. Kim, Z. Cao, W. Tan, *Proc. Natl. Acad. Sci. U.S.A.* **2008**, *105*, 5664–5669.
[30] C. J. Bracken, S. A. Lim, P. Solomon, N. J. Rettko, D. P. Nguyen, B. S. Zha, K. Schaefer, J. R. Byrnes, J. Zhou, I. Lui, et al., *Nat. Chem. Biol.* **2021**, *17*, 113–121.
[31] Tolle, F. & Mayer, G. *Methods Mol. Biol.* **2016**, *1380***,** 77–84.
[32] Zuker, M. *Nucleic Acids Res.* **2003**, *31***,** 3406–3415.
[33] K.K. Chan, D. Dorosky, P. Sharma, S.A. Abbasi, J. M. Dye, D.M. Kranz, A.S. Herbert, E. Procko, *Science* **2020**, *369***,** 1261–1265.
[34] M. Hoffmann, H. Kleine-Weber, S. Schroeder, N. Krüger, T. Herrler, S. Erichsen, T.S. Schiergens, G. Herrler, N.-H. Wu, A. Nitsche *et al. Cell **2020**, 181***,*** 271–280.e8.

10.1002/anie.202100316

Table 1 – Kinetic properties of the aptamers SP5, SP6 and SP7 measured by surface plasmon resonance.

Sequence	Condition	k_a ($10^4 M^{-1}s^{-1}$)	k_d ($10^4 s^{-1}$)	K_D (nM)
SP5	37°C	1 ± 0.2	37 ± 36	9.2 ± 7.9
SP6	37°C	2.1 ± 0.6	4.5 ± 1.9	21 ± 4.6
SP7	37°C	1.5 ± 0.4	2.9 ± 1.2	18.9 ± 5.5
SP5	25°C	1.19 ± 0.1	1.74 ± 0.01	14.7 ± 0.8
SP6	25°C	2.5 ± 0.3	3.4 ± 0.2	13.9 ± 0.6
SP7	25°C	1.3 ± 0.2	1.7 ± 0.7	13.1 ± 3.8

10.1002/anie.202100316

ToC

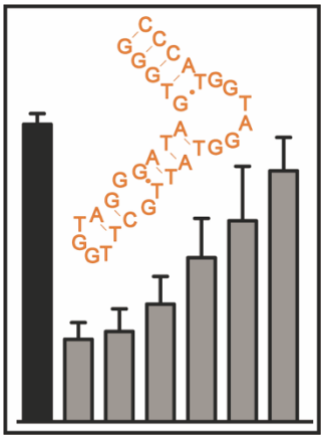

SP6 is a DNA aptamer binding to the SARS-CoV-2 spike glycoprotein and inhibits pseudovirus infection of cells. As the aptamer does not interfere with the CoV-2S ACE2 receptor binding domain it provides an RBD-independent mechanism of virus inhibition.

Keywords: aptamers, SELEX, SARS-CoV-2, antiviral, coronavirus